Proceedings of the Institute of Acoustics

NONLINEAR ACOUSTICS IN MEDICAL ULTRASOUND

Andrew C Baker

School of Physics, University of Bath, Bath, BA2 7AY, U.K.

1. INTRODUCTION

Ultrasound was first used diagnostically in medicine in the mid 1960s. Today it is used extensively in a wide variety of medical applications ranging from diagnostic imaging (including Doppler) to therapy such as hyperthermia and lithotripsy (stone breaking). Diagnostic imaging systems typically operate in a pulse-echo mode with a centre frequency (f_0) in the range 1 to 10 MHz. Almost all diagnostic systems employ some form of focusing, either in the form of a lens or electronic beam forming and often both. Duck et al [1] presented a variety of data in a survey of diagnostic systems indicating that peak positive pressures (P+) for such systems were in the range 0.75 to 8.8 MPa and peak negative pressures (P-) were in the range 0.10 to 3.90 MPa. In a recent paper [2] that examined trends in acoustic output it was noted that there had been a steady increase in the output of diagnostic equipment over the last 20 years. A survey of lithotripsy systems [3] showed that typically these have centre frequencies in the range from 150 kHz to over 850 kHz with peak positive pressures in the range 9 to 105 MPa and peak negative pressures between 2.8 to 9.9 MPa. These combinations of high acoustic pressures, high frequencies and the use of focusing mean that all medical ultrasound systems (therapeutic and diagnostic) operate in regimes where nonlinear effects are very significant but it is only relatively recently that this has been recognized.

In the early days of medical ultrasound scanners it was generally assumed that they behaved as linear systems. It was about 1980 when the experience of nonlinearity in other branches of acoustics started to be applied to medical ultrasound. In particular Muir and Carstensen [4] highlighted some of the nonlinear effects that were of potential interest in medical ultrasound. A companion paper [5] presented experimental measurements which were aimed, at least partially, at convincing those sceptics in biomedical research that nonlinear effects really did occur in medical ultrasound. It is noticeable that the measurements presented were in terms of intensity and fundamental amplitude; no time waveforms were produced. The authors noted that a hydrophone with a flat frequency response had been reported in the literature but that they were "difficult to construct and not commercially available". In the absence of such hydrophones Carstensen et al [5] were unable to produce any hard evidence for nonlinear distortion in diagnostic ultrasound but concluded that "harmonic distortion and formation of shock waves may occur in many of the highly focused ultrasonic beams used in these devices".

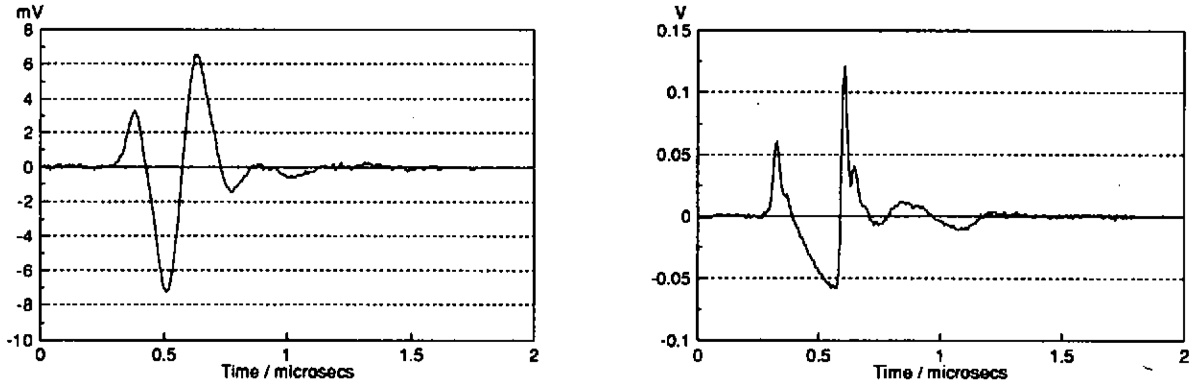

Fig. 1: Typical ultrasonic pulses from a medical ultrasound system; (a) low drive level (b) high drive level (+20 dB)

It was only in the early 1980s when polyvinylidene difluoride (pvdf) membrane hydrophones [6] became available that time waveforms such as those of Fig. 1(b) became commonplace in the literature and there followed a widespread acceptance of nonlinearity in medical ultrasound systems. Fig. 1 shows the distortion observed experimentally in an initially sinusoidal waveform as the drive level is increased. The transducer was a 3.5 MHz, 13 mm diameter medical imaging transducer. The hydrophone was a Marconi pvdf membrane positioned co-axially 200 mm from the transducer. The increase in drive level between (a) and (b) is 20 dB. At low drive (a) the initial waveform is a sinusoidal pulse whose peak positive pressure (P+) and peak negative pressure (P-) are comparable as are the slopes of the waveform in the compressional and rarefactional phases. The distorted waveform (b) however shows a marked top-bottom asymmetry and a much steeper compressional phase in comparison to the rarefactional phase. This is characteristic of the distortion caused by nonlinear propagation as observed in medical ultrasound systems. The distorted waveform does contain one feature which is only indirectly caused by nonlinear propagation, that is the ringing at about 20 MHz which is particularly pronounced on the rarefactional side of the largest positive half cycle. This ringing is due to a resonance of the hydrophone and is discussed further in the next section. It is relatively easy to show that the distortion arises from nonlinear propagation in the medium (water) by repeating the measurements close to the transducer where no distortion would be observed as the drive level is increased.

Although it is now known that diagnostic medical ultrasound systems can generate nonlinear effects in water [7] and in tissue [8] there has been little change in the way that such systems are analysed since the theoretical treatments of nonlinear propagation are neither common nor easily implemented. In the following sections some of the problems of measurement and characterisation are discussed and some of the theoretical methods of predicting medical ultrasound output are reviewed.

2. MEASUREMENT AND CHARACTERISATION OF NONLINEAR FIELDS

2.1 Hydrophone frequency response

The main problem in measuring the acoustic output of medical ultrasound systems arises from the wide bandwidth that is generated by nonlinear distortion. A plane sinusoidal wave will distort to become a saw-tooth whose harmonic amplitudes vary as 1/n where n is the harmonic number. In general this 1/n fall off will be observed in all strongly shocked waveforms. It is therefore important that the hydrophone bandwidth is as wide as possible and preferably fairly flat. Fig. 2 shows the magnitudes of a Fast Fourier Transform (FFT) of the two waveforms in Fig. 1. At the low drive level (Fig. 2a) almost all the energy is in a single peak centred around 3.5 MHz, the centre frequency of the transducer.

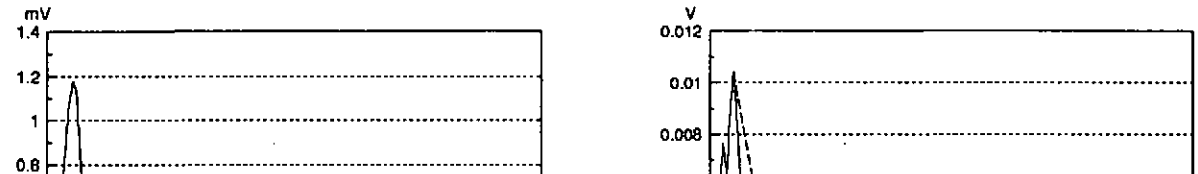

Fig. 2: Spectral magnitudes of time waveforms in Fig. 1; (a) low drive level (b) high drive level (+20 dB), dashed line indicates 1/f fall off in amplitude.

As the drive is increased (Fig. 2b) the distortion causes peaks to appear in the spectrum at multiples of the centre frequency. This is analogous to harmonic generation in the continuous wave (CW) case. In the high drive case the spectral magnitudes show two artifacts caused by the hydrophone response. These can be seen by comparing the measured magnitudes with the dashed line which indicates a 1/f fall-off starting from the centre frequency. First there is little signal above 30 MHz and second the amplitudes are higher than expected around 20 MHz, the reasons for this are apparent in the hydrophone frequency response (Fig. 3).

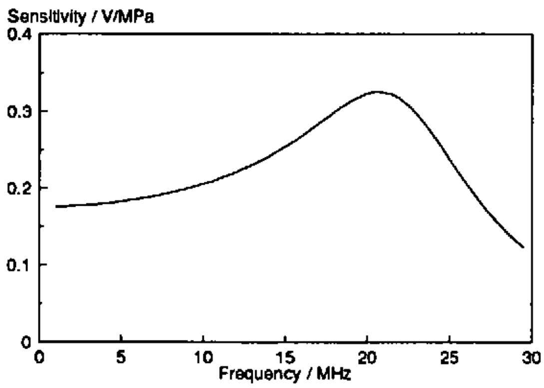

Fig. 3: Predicted membrane hydrophone response.

The two main factors that dominate the hydrophone response are the thickness resonance of the membrane and cable resonance. The effect of the cable resonance can be minimised by reducing the cable length. The hydrophone used here (made by GEC Research) had two pvdf films (25 micron thick) laminated together and its main resonance corresponded to the membrane being half a wavelength thick at the resonant frequency (about 20 MHz). The response then falls off rapidly beyond this.

In theory it should be possible to deconvolve the hydrophone response from the waveform. In practice it is difficult to determine the magnitude and phase of the hydrophone transfer function over a sufficiently wide bandwidth. An alternative approach is to use a hydrophone amplifier that has a frequency response that starts to fall off at around the hydrophone resonance, thus extending the flat region of the response. This does introduce other potential problems such as accurate characterisation of the amplifier and the possibility of the amplifier saturating when large signals are applied. The effect of the thickness resonance can also be reduced by using a thinner membrane. GEC Marconi have produced such devices with a single film of 9 μm thickness. The main drawback of these (coplanar) hydrophones is the need to use distilled, de-ionised water as the measurement medium to prevent electrical coupling between the two sides of the membrane. In the bilaminar hydrophone the earth connection for each pvdf film is on the outside so there is no need for de-ionised water. Other hydrophone types are available such as pvdf needle probes which tend to have a poorer higher frequency response when compared to the pvdf membrane hydrophones and ceramic probe hydrophones which tend to be rather more resonant than pvdf membranes. Smith [9] illustrates these points in a comparison of a number of hydrophones with particular reference to their use in medical ultrasound fields. In general hydrophone linearity should also be considered but pvdf is essentially linear so should not cause any problems.

Although nonlinear effects cause measurement problems by virtue of the wide bandwidth of distorted signals it can be used to good effect in the calibration of hydrophones. The National Physical Laboratory (NPL) routinely uses nonlinear distortion to allow the calibration of hydrophones at integer multiples of 1

MHz up to 20 MHz. A strongly shocked waveform (with a fundamental frequency of 1 MHz) is recorded using a secondary standard hydrophone. The device to be calibrated is then substituted and the outputs compared [10].

2.2 Hydrophone size and positioning

An important consideration for hydrophones in medical ultrasound is size. Fundamental frequencies for imaging systems tend to fall in the range 1 to 10 MHz giving wavelengths in water of 1.5 to 0.15 mm. The fundamental beamwidths are typically a few millimetres or less hence in order to resolve the spatial detail of these pressure fields hydrophone sizes need to be of the order of 1 mm or less. The harmonics however are generated with narrower beamwidths than the fundamental as can be seen in Fig. 4 which shows a section through the focal plane of a focused CW ultrasound beam. In the focal plane we observe the same sort of directivity pattern for the fundamental that would be observed in the farfield of a plane circular radiator (ie $2J_1(x)/x$). The harmonic beams get narrower and the sidelobe levels get lower with increasing harmonic number. In the central part of the beam it is found that the beam pattern for the n^{th} harmonic varies as the fundamental beam pattern to the n^{th} power. This corresponds to -3 dB beamwidths for the harmonics that vary as $1/\sqrt{n}$. It should be noted that Fig. 4 corresponds to conditions of only moderate nonlinearity. At higher drive levels the fundamental amplitude would be reduced in the main lobe due to the transfer of energy to higher harmonics and would ultimately become saturated. One of the implications of the narrower harmonic beamwidths is that the harmonic amplitudes will be averaged across active area the hydrophone. This will cause the peak positive pressure to under-estimated. Gallantree and Smith [11] showed that in certain circumstances this could lead to errors of 50% or more in the peak positive pressure (P+).

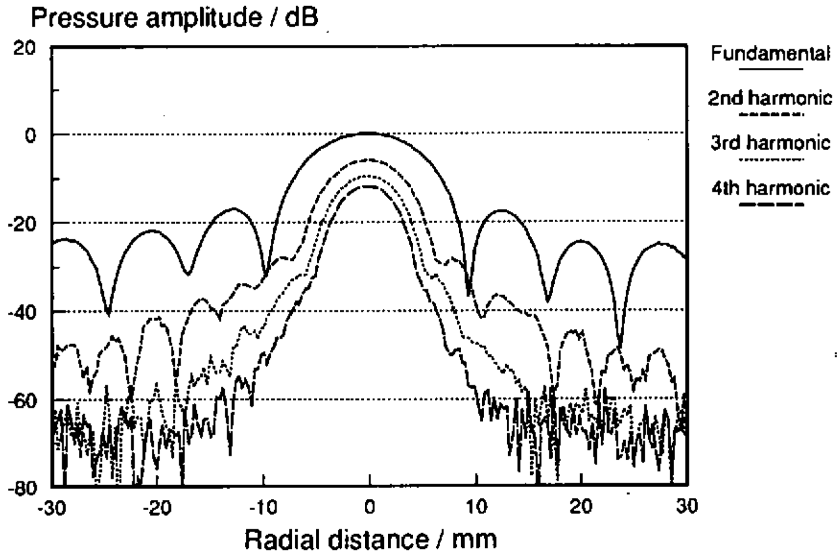

Fig. 4: Measured radial pressure variation of harmonics. Fundamental frequency = 2.25 MHz, axial range = focal distance = 440 mm, aperture radius = 19 mm.

The narrow beamwidths of the harmonics also necessitate accurate alignment of the source transducer and accurate positioning of the hydrophone. This is often done with micro-manipulators or stepper motor assemblies. An alternative approach to accurate positioning of a single hydrophone is to use an array of closely spaced hydrophones as found in the NPL Ultrasonic Beam Calibrator (UBC) [12]. Other methods for measuring the output of medical ultrasound systems include radiation force balances [13] and RF power meters [14].

2.3 Characterisation of ultrasound systems

Given that it is possible to find a hydrophone that will faithfully reproduce the acoustic pressure the next problem is deciding how to characterise the output of medical ultrasound systems. A few of the more commonly used parameters are described below but nonlinearity causes a very significant problem here; a measurement taken at one particular drive level can not be scaled to represent another drive level. Similarly measurements made at one position in the field cannot be translated (easily) to give information about another position in the field with a different geometry. One solution to this problem is only to measure parameters at the location where they have their maximum and for the highest drive levels. This is only a partial solution since it only partially describes the pressure field and in any case it is found that for instance the position where the peak positive pressure occurs in the field is usually different to the position where the peak negative pressure occurs.

Another consideration in choosing the parameters to characterise medical ultrasound systems is their relation, if any, to the onset of biological effects. A number of possible mechanisms for bio-effects exist (e.g. cavitation, heating, mechanical shear and streaming) but their relative contributions are not always clear, hence it is not easy to indicate which output parameters should be minimised to reduce the likelihood of bio-effects. Currently there is evidence of a threshold for biological damage by heating. There are no confirmed reports of adverse effects in living mammals from increases in body temperature of 1 °C or less and serious damage can result from prolonged elevation of the body temperature by 2.5 °C or more [15]. For further reading a range of bio-effects papers can be found in a special issue of Ultrasonics [16] and a review of the epidemiology of ultrasound exposure can be found in Ref. 17.

The most directly observable quantity is the pressure waveform but owing to nonlinear distortion and the top-bottom asymmetry there are a range of parameters that might be significant, for example: peak positive pressure, peak negative pressure, rise time, pulse length, fundamental amplitude etc. There are also many derived quantities that could be used such as intensity (pulse average, temporal average, spatial average). A recent standard [18] from the International Electrotechnical Commission (IEC) identifies three acoustic parameters as important in characterising diagnostic ultrasound. The parameters chosen are; the peak negative pressure (P-), the spatial peak, temporal average intensity (I_{spta}) and the output beam intensity (I_{ob}). The standard, amongst other things, sets levels for these parameters below which no declaration of output levels is required and clinically such systems could be considered as totally safe for any application. The proposed thresholds are 1 MPa for P-, 100 mW/cm^2 for I_{spta} and 20 mW/cm^2 for I_{ob}. This is in broad agreement with a statement from the American Institute of Ultrasound in Medicine (AIUM) [15] which points to the lack of any confirmed biological effects in mammalian tissues exposed in vivo to unfocused ultrasound with intensities (I_{spta}) below 100 mW/cm^2 or to focused ultrasound with intensities below 1 W/cm^2.

A parameter that gives some indication of the degree of distortion is the plane wave shock parameter $\sigma = \beta\varepsilon kx$. ($\beta$ is the nonlinearity parameter of the medium (3.5 for water at 20 °C), ε is the acoustic Mach number i.e. the particle velocity divided by the propagation velocity, k is the wavenumber and x is the distance travelled by the wave). A value of σ=1 indicates the stage at which a vertical discontinuity is just starting to form, at this stage the distance (x) is known as the plane wave shock distance (l_D), i.e. $l_D = 1/(\beta\varepsilon k)$. The plane wave shock parameter and shock distance must be used with caution in the diffractive fields of real ultrasonic sources since they take no account of the spatial variation of the pressure field. In an attempt to allow for focusing gains and diffraction in medical ultrasound systems a variant of the shock parameter known as σ_m has also been defined [19]

To add to the difficulties of acoustic characterisation even determination of parameters like the effective aperture radius, amplitude shading and focal length is not trivial. Even when it is possible to disconnect the transducer from the system and drive it CW at low amplitude it is not easy to accurately characterise the source [20,21,22]

The choice of medium for calibration and bio-effects experiments is also important. Water is well characterised, readily available and easy to work with but has the drawback that high levels of nonlinear distortion occur because it has a low absorption coefficient in comparison with tissue (at frequencies of interest). In addition the frequency dependence of absorption in water is higher than in tissue (square law as opposed to roughly linear). Such factors are highly significant when nonlinear distortion is present as it is often the high frequency absorption that ultimately limits the generation of harmonics and hence the maximum pressures observed. A number of alternatives are available; fluids such as castor or silicone oil provide higher absorption than water and are relatively easy to work with. Tissue mimic gels can be acoustically closer to tissues than oils but are not easy to use as it is difficult to position and move hydrophones. To compound the problem many tissues are not well characterised acoustically, especially not over the wide range of frequencies generated by highly distorted ultrasound. Nonlinear effects can also cause absorption measurements to become dependent on the acoustic drive level [23,24] and the position of the sample in the field [24].

3. THEORETICAL PREDICTIONS OF NONLINEAR EFFECTS

The complexity of nonlinear propagation and medical ultrasound systems indicate that it is unlikely that an accurate theoretical solution will be simple. It seems sensible then to investigate a variety of theoretical models that range from the fully accurate but computationally intensive to the more approximate but easily implemented models.

One dimensional solutions to the nonlinear wave equation, such as those of Blackstock [25], can provide some useful information for medical ultrasound systems but are unable to reproduce the fine detail and phase variations seen in "real" pressure fields. Highly diffracted and focused pressure fields require more rigourous treatment. Smith and Beyer [26] commented on the "lack of appropriate theoretical analysis" when they published nonlinear measurements on a focused acoustic source operated at 2.3 MHz. One of the most significant theoretical advances came in 1969 when Zabolotskaya and Khokhlov [27] published a solution of the nonlinear wave equation for a confined sound beam in which it was assumed that "the shape of the wave varies slowly both along the beam and transversely to it". In 1971 Kuznetsov [28] extended their treatment to include absorption and the resulting equation is now widely known as the KZK equation after its originators. The solution is also known as the parabolic approximation to the nonlinear wave equation and is equivalent to the paraxial approximation used in optics. The KZK equation accounts for diffraction, absorption and nonlinearity, and it is valid for circular apertures that are many wavelengths in diameter and will accept arbitrary source conditions.

In 1983 Lucas and Muir [29] published a perturbation solution for the second harmonic component of a focused aperture. Their solution was based on the KZK equation and was valid for quasi-linear drive levels, i.e. it was assumed that there was sufficient nonlinearity to generate some second harmonic without affecting the fundamental amplitude significantly. At about the same time a group from Bergen University, Norway [30] published numerical results based on a frequency domain solution of the KZK equation under conditions of strong nonlinearity. The solution accounted for any number of harmonics and the transfer of power between harmonics and so it was possible to predict effects like saturation of the fundamental. Comparisons of the numerical solution to the KZK with experimental measurements have shown it to predict accurately pressure fields similar to those generated by diagnostic ultrasound. Continuous wave pressure fields for both plane [31] and focused sources [32] show good agreement for peak pressures up to about 1 MPa. Figure 5 compares experimental measurements with the numerical solution of the KZK equation along the axis of a focused radiator operating at 2.25 MHz. Although the acoustic source used had a larger diameter and longer focal length than those used in diagnostic ultrasound, the focal gain (G) given by the Rayleigh distance ($ka^2/2$) divided by the focal length (D) is comparable with diagnostic systems. The advantage of this slight scaling up is that the spatial variations in the pressure field are easier to monitor with a 1 mm diameter hydrophone. In Fig. 5 there is good agreement between experiment and theory for the fundamental and harmonics up to the fourth, data for higher harmonics is not plotted for clarity. Corresponding phase plots also show good agreement.

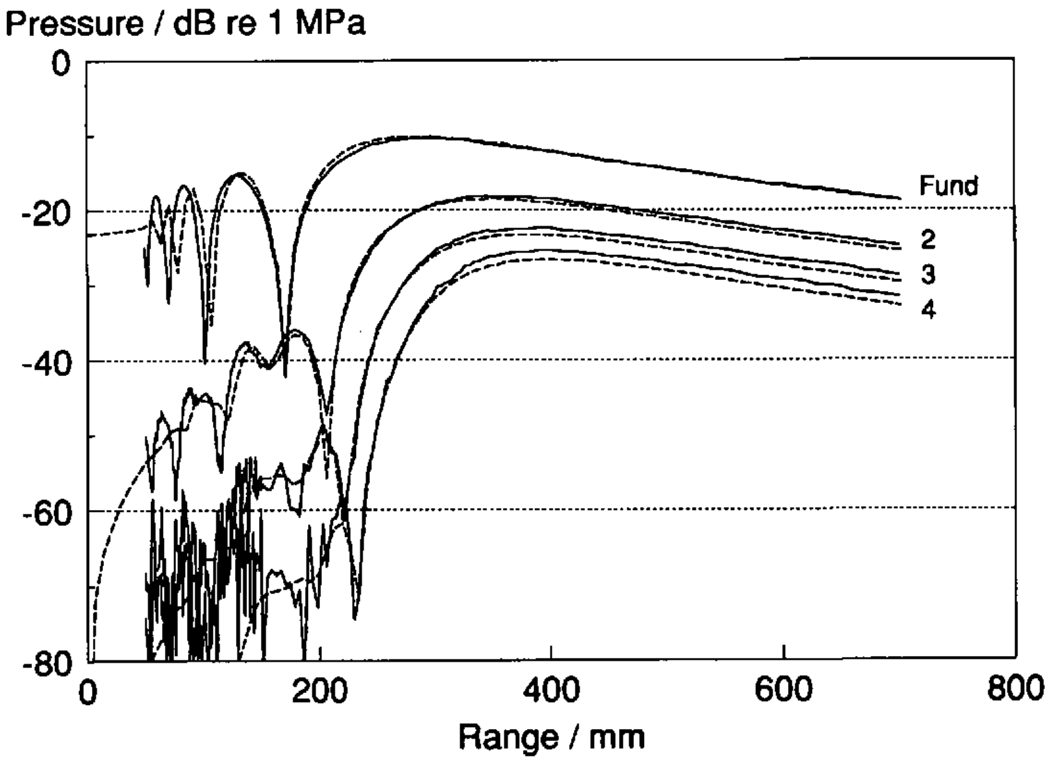

Fig. 5: Axial pressure for focused CW source, fundamental to fourth harmonic; fundamental frequency 2.25 MHz, 19 mm radius, 440 mm focal length, gain 3.9. (— Experiment, - - Theory).

The numerical solution has also been adapted for pulsed fields and compared favourably with measurements on pulsed systems [22,33]. Figure 6 shows the measured and predicted waveforms and spectral magnitudes for a pulsed, focused radiator with dimensions similar to those used in medical ultrasound systems. Crucial to the good agreement seen in Figures 5 and 6 was the availability of a well characterised acoustic source. The main difficulty in modelling "real" diagnostic fields is determining the initial source conditions [22] i.e. the initial waveform, the source aperture and shading and the geometric focal length. The parabolic approximation imposes some limitations on the allowed geometries. Sources similar to those typically used in diagnostic ultrasound can be modelled accurately for field points that are less than about 20 degrees off the acoustic axis. At short ranges the aperture half-angle subtended by the field point shoul also be less than about 20 degrees. This can be a serious limitation in lithotripsy fields where the aperture angle can be as great as 45 degrees.

The numerical solution of the KZK is limited to some extent by computer processor time. The higher the required drive pressure then the more harmonics that are needed in the solution, this in turn increases the processor time. If too few harmonics are included then energy remains trapped at lower frequencies and distorts the spectrum. The required spatial resolution also affects the processor time since the solution operates on a finite difference grid and if the grid points are closely spaced then more points are needed and hence more processor time. Fig. 5 shows the effect of the grid resolution as the theoretical solution starts smoothing the more rapid axial pressure variations that are found closer to the source (i.e. at ranges less than 100 mm). Further details of the solution to the KZK equation that was used to generate the theoretical predictions of Figs. 5 and 6 are given in the Appendix.

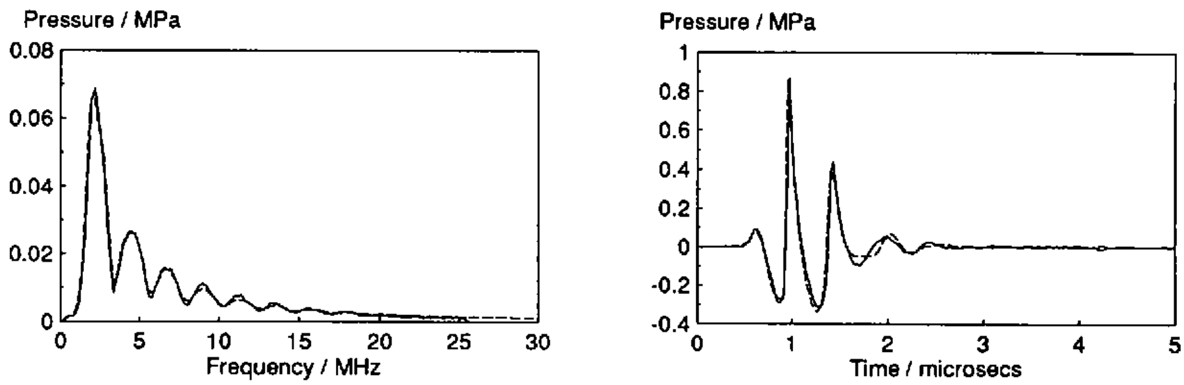

Time waveform Spectral magnitudes

Fig. 6: Pulsed pressure field at axial range of 300 mm for focused source; 19 mm radius, 440 mm focal length (— Experiment, - - Theory)

A recent new approach to modelling pressure fields due to circular apertures is that of Christopher and Parker [34] who use a plane wave spectrum approach and discrete Hankel transforms to calculate diffraction effects. Their solution is not limited by the parabolic approximation and shows good agreement with previous measurements and solutions. Another approach has been to assume that the radial pressure field has a Gaussian profile. Although this doesn't predict the near field features that a full diffraction model would show it does reduce the computer processor time required. Dalecki et al [35] used a Gaussian beam model to predict heating rates due to the absorption of finite amplitude ultrasound on the acoustic axis of a focused transducer. They reduced the theoretical solution to an analytical form and showed agreement with experimental measurements of heating rate.

4. SUMMARY

Medical ultrasound systems ranging from diagnostic imaging systems to lithotripters operate under acoustic regimes where nonlinear effects are very significant. It is necessary to make allowances for this in both the way that measurements are made and in the application of theoretical models. It is essential to characterise the acoustic source carefully in order to provide accurate initial conditions for numerical models. Currently good predictions are available for simple sources operating CW or pulsed in water with some restrictions on geometry. More work is required for accurate in vivo predictions for both diagnostic and therapeutic medical ultrasound systems.

APPENDIX: NUMERICAL SOLUTION OF THE KZK EQUATION

LIST OF SYMBOLS

a - aperture radius.
b - diffusivity of sound ($=2\alpha c k^2$).
c - speed of sound (1486 m/s for water at 20°C).
f - frequency. (f_o - fundamental frequency).
G - focusing gain (= R_o/D).
g - Fourier coefficient in solution.
h - Fourier coefficient in solution.
j - $\sqrt{-1}$.
k - wavenumber ($=2\pi/\lambda$).
l_D - shock distance ($=1/\beta\varepsilon k$).
n - harmonic number.
p - acoustic pressure (= P - P_o).
p_o - acoustic pressure at the source.
P - total pressure (static + acoustic).
P_o - static pressure.
P+ - peak positive pressure.
P- - peak negative pressure.
q - Fourier solution amplitude.
R_o - Rayleigh distance (= $ka^2/2$).
r - radial coordinate.
t - time.
u - particle velocity.
u_o - particle velocity at the source.
z - axial coordinate.
α - absorption coefficient (2.5×10^{-15} Np $m^{-1}Hz^{-2}$ for water).
β - parameter of nonlinearity (3.5 for water at 20°C).
Γ - shock parameter ($=\beta\varepsilon k/\alpha$).
ε - acoustic Mach number (= u/c).
ζ - normalised radial coordinate (= r/a).
θ - harmonic phase.
λ - wavelength (= c/f).
σ - normalised axial coordinate (= z/R_o) or shock parameter ($=\beta\varepsilon k x$).
τ - retarded time ($=\omega t - kz$).
ω - angular frequency (= $2\pi f$).
Φ - scalar velocity potential.
Ψ - Fourier solution phase.
∇ - gradient operator.
∇_t - transverse gradient operator.

A1 General wave equation

Following the work of Zabolotskaya and Khokhlov [27], Kuznetsov [28] derived a nonlinear wave equation for a scalar potential, Φ, by considering the dynamics of a viscous, heat conducting fluid. The equation was correct to the second order with terms for diffraction, absorption and nonlinearity:

$$\frac{\partial^2\Phi}{\partial t^2}-c^2\nabla^2\Phi=\frac{\partial}{\partial t}\left[2\alpha c k^2\nabla^2\Phi+(\nabla\Phi)^2+\frac{B}{2A}\frac{1}{c^2}\left(\frac{\partial\Phi}{\partial t}\right)^2\right] \qquad 1$$

The left-hand side of equation 1 is the three dimensional linear wave equation, of the three terms on the right-hand side the first term is a linear term and accounts for absorption, the second term is due to convective nonlinearity and the third is due to nonlinearity in the equation of state.

A2 Parabolic approximation

Kuznetsov also showed that the equation (1) could be simplified, by approximation, in the case of a quasi-plane wave field and the Laplacian (∇^2) can be replaced by the transverse Laplacian ($\nabla_\perp^2$). A circular aperture that is many wavelengths in diameter (i.e ka is large) falls in this category since most of the energy is confined to a beam in the axial direction. This is known as the parabolic (or paraxial) approximation and is equivalent to the Fresnel approximation that is sometimes used in the diffraction integral for near-field calculations. Kuznetsov's parabolic approximation can be expressed in a normalised form [36]:

$$\left(4\frac{\partial^2}{\partial\tau\partial\sigma}-\nabla_\perp^2-4\alpha R_o\frac{\partial^3}{\partial\tau^3}\right)\bar{p}=2\frac{R_o}{l_D}\frac{\partial^2}{\partial\tau^2}\bar{p}^2 \qquad 2$$

where $\bar{p}$ (= p/p_o) is the acoustic pressure normalised by the source pressure and $\tau(=\omega t-kz)$ is the retarded time, i.e. includes a phase term for a plane wave travelling in the z direction. In this equation σ is the axial coordinate normalised by the Rayleigh distance (not the shock parameter) and ζ is the radial coordinate normalised by the aperture radius, i.e.

$$\sigma=\frac{2z}{ka^2} \text{ and } \zeta=r/a$$

A trial solution was then assumed in the form of a Fourier series (for the time waveform) with amplitude and phase that were functions of the spatial coordinates, i.e.

$$p(\sigma,\zeta,\tau)=\sum_{n=1}^{\infty}q_n(\sigma,\zeta,\tau)\sin(n\tau+\psi_n(\sigma,\zeta,\tau)) \quad \text{or}$$

$$p(\sigma,\zeta,\tau)=\sum_{n=1}^{\infty}g_n(\sigma,\zeta,\tau)\sin(n\tau)+h_n(\sigma,\zeta,\tau)\cos(n\tau) \qquad 3$$

where $g_n=q_n\cos\psi_n$, $h_n=q_n\sin\psi_n$

and n is the harmonic number, with n=1 representing the fundamental frequency. Substituting the trial solution (3) into equation 2 and collecting terms in $\sin(n\tau)$ and $\cos(n\tau)$ gives a set of coupled differential equations for g_n and h_n:

$$\frac{\partial g_n}{\partial\sigma}=-n^2\alpha R_o g_n+\frac{1}{4n}\nabla_\perp^2 h_n+\frac{nR_o}{2l_D}\left(\frac{1}{2}\sum_{k=1}^{n-1}(g_k g_{n-k}-h_k h_{n-k})-\sum_{p=n+1}^{\infty}(g_{p-n}g_p+h_{p-n}h_p)\right) \qquad 4$$

$$\frac{\partial h_n}{\partial\sigma}=-n^2\alpha R_o h_n+\frac{1}{4n}\nabla_\perp^2 g_n+\frac{nR_o}{2l_D}\left(\frac{1}{2}\sum_{k=1}^{n-1}(h_k g_{n-k}+g_k h_{n-k})+\sum_{p=n+1}^{\infty}(h_{p-n}g_p-g_{p-n}h_p)\right) \qquad 5$$

These equations were then solved numerically.

A3 Numerical solution

Equations 4 and 5 form the basis of the numerical solution which was implemented by Aanonsen in a FORTRAN program called FOCAB [37]. Standard numerical approximations were used for the derivatives and the pressure field was calculated using a finite difference technique. The harmonic coefficients (g_n and h_n) were represented by pairs of two-dimensional grids, one such grid is shown in Figure A1.

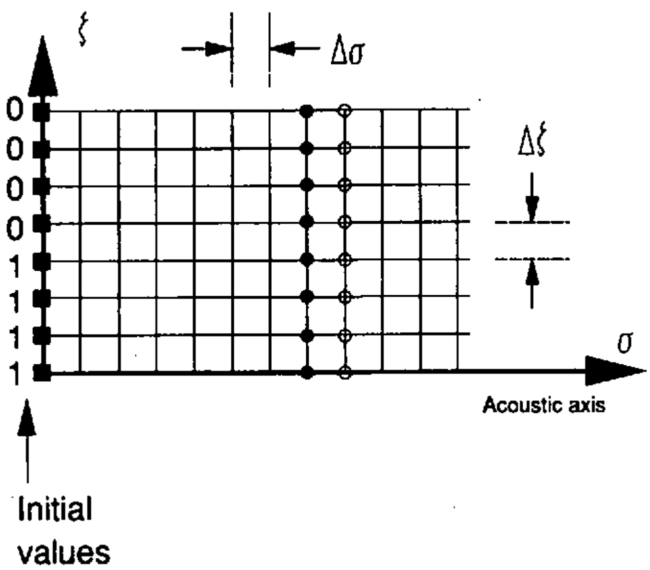

Fig. A1: Simplified finite difference grid.

Thus if the filled circles of Figure A1 represent the current values of g_n in the radial direction, then equation 4 relates them to the next set of values along the acoustic axis (denoted by the empty circles). The numerical scheme replaces the partial derivatives of equation 4 with small increments, e.g.

$$\frac{\partial g_n}{\partial \sigma} \text{ becomes } \frac{g'_n - g_n}{\Delta\sigma}$$

where g'_n is the new value of g_n. Similar numerical approximations were used to replace the transverse gradient operator and the resulting equations were solved to give the change in the harmonic component $(g'_n - g_n)$ for a small step ($\Delta\sigma$) in the axial direction. The initial conditions were given by the radial pressure distribution across the piston face and baffle (represented by the filled squares in Fig A1). The physical meaning of the scheme described by equations 4 and 5 can be seen more clearly if the equations are written in a slightly different form. If we take equation 4 and express it in terms of the original z coordinate we get an expression for the change in g_n with axial range (z):

$$\frac{\partial g_n}{\partial z} = -n^2\alpha g_n + \frac{1}{4nR_o}\nabla_1^2 h_n + \frac{n}{2l_D}\left(\frac{1}{2}\sum_{k=1}^{n-1}(g_k g_{n-k} - h_k h_{n-k}) - \sum_{p=n+1}^{\infty}(g_{p-n}g_p + h_{p-n}h_p)\right) \qquad 6$$

This shows that the change in the field g_n with distance along the z axis is due to three terms:

Attenuation.
This term has an n^2 dependence (i.e. it varies with the square of the frequency) and is proportional to α (the absorption coefficient); thus we have the classic frequency squared dependence of absorption in a fluid.

Diffraction.
This term has a reciprocal dependence on nR_o; thus diffraction becomes less important as the frequency (or harmonic number) increases and as the aperture radius increases. In other words, the more wavelengths across the aperture the more the beam looks like a plane wave travelling in the z direction. Diffraction also depends on the transverse gradient, with rapid changes in the field in the radial direction giving rise to large diffraction terms, such as occur at the piston edge. It was implicit in the initial assumptions that the field would be quasi-plane wave; hence the absence of the longitudinal term in the gradient operator.

Nonlinearity.
The nonlinear term is proportional to n, hence nonlinearity becomes more important with increasing frequency. It also depends on the reciprocal of l_D, the plane wave shock distance.

The nonlinear term is the only coupling term in the equation, i.e. it intermixes terms of different harmonic number. If the products under the summations are evaluated it is found that they pick out all combinations of harmonics that have sum or difference equal to the harmonic (n) in question. For example in evaluating the fourth harmonic the nonlinear term involves products of the following harmonics: 1 and 3, 2 and 2, 1 and 5, 2 and 6, 3 and 7 ... etc. This term is also the only one with any connection with the drive level (p_o) so small signal runs were achieved by reducing the pressure across the piston face, and hence the Mach number so that nonlinear generation became insignificant.

A similar result to equation 6 is obtained from equation 5 for the change in h_n along the axis.

REFERENCES

[1] F A DUCK, H C STARRITT, J D AINDOW, M A PERKINS & A J HAWKINS, 'The output of pulse-echo ultrasound equipment: a survey of powers, pressures and intensities', Brit J Radiol, 58 p989 (1985)

[2] F A DUCK & K MARTIN, 'Trends in diagnostic ultrasound exposure', Phys Med Biol, 36 p1423 (1991)

[3] A J COLEMAN & J E SAUNDERS, 'A survey of the acoustic output of commercial extracorporeal shock wave lithotripters', Ultrasound Med and Biol, 15 p213 (1989)

[4] T G MUIR & E L CARSTENSEN, 'Prediction of nonlinear acoustic effects at biomedical frequencies and intensities', Ultrasound Med and Biol, 6 p345 (1980)

[5] E L CARSTENSEN, W K LAW, N D McKAY & T G MUIR, 'Demonstration of nonlinear acoustical effects at biomedical frequencies and intensities', Ultrasound Med and Biol, 6 p359 (1980)

[6] D R BACON, 'Characteristics of a pvdf membrane hydrophone for use in the range 1-100 MHz', IEEE Trans Sonics Ultrasonics, SU-29 p18 (1982)

[7] F A DUCK & H C STARRITT, 'Acoustic shock generation by ultrasonic imaging equipment', Brit J Radiol, 57 p231 (1984)

[8] H C STARRITT, M A PERKINS, F A DUCK & V F HUMPHREY, 'Evidence for ultrasonic finite-amplitude distortion in muscle using medical equipment', J Acoust Soc Am 77 p302 (1985)

[9] R A SMITH, 'The importance of the frequency response of a hydrophone when characterising medical ultrasound fields', Proc Inst Acoust 8 (Part 2) p119 (1986)

[10] R A SMITH & D R BACON, 'A multiple-frequency hydrophone calibration technique', J Acoust Soc Am, 87 p2231 (1990)

[11] H R GALLANTREE & R A SMITH, 'Small area membrane hydrophones', IEEE Ultrasonics Symposium p761 (1987)

[12] R C PRESTON, 'The NPL Ultrasound Beam Calibrator', IEEE Trans UFFC, 35 p122 (1988)

[13] M J FARMERY & T A WHITTINGHAM, 'A portable radiation force balance for use with use with diagnostic ultrasound equipment', Ultrasound Med and Biol, 3, p373 (1978)

[14] K MARTIN, 'Measurement of acoustic output parameters from medical ultrasound devices with an RF power meter system', IEEE Trans UFFC, 35 p140 (1988)

[15] AIUM, 'Bioeffects considerations for the safety of diagnostic ultrasound', J Ultrasound Med 7 Supplement (1988)

[16] Ultrasonics 28, 1990. (Special bio-effects issue)

[17] M C ZISKIN & D B PETITTI, 'Epidemiology of human exposure to ultrasound: a critical review', Ultrasound Med and Biol, 14 p91 (1988)

[18] IEC Publication 1157:1992, 'Requirements for the declaration of the acoustic output of medical diagnostic ultrasound equipment', (1992)

[19] IEC Publication 1102:1991, 'Measurement and characterisation of ultrasonic fields using hydrophones in the frequency range 0.5 MHz to 15 MHz', (1991)

[20] J ADACH & R C CHIVERS, 'A detailed investigation of effective geometrical parameters for weakly focussed ultrasonic transducers. Part I: Optimisation of experimental procedures', Acustica 70, p12 (1990)

[21] J ADACH & R C CHIVERS, 'A detailed investigation of effective geometrical parameters for weakly focussed ultrasonic transducers. Part II: A systematic study including an absorbing medium', Acustica 70, p135 (1990)

[22] A C BAKER, 'Prediction of nonlinear propagation in water due to diagnostic medical ultrasound equipment', Phys Med Biol, 36, p1457 (1991)

[23] S A GOSS & F J FRY, 'Nonlinear acoustic behaviour in focused ultrasonic fields: Observations of intensity dependent absorption in biological tissue', IEEE Trans Sonics Ultrasonics SU-28, p21 (1981)

[24] B ZEQIRI, 'Errors in attenuation measurements due to nonlinear propagation effects', J Acoust Soc Am 91, p2585 (1992)

[25] D T BLACKSTOCK, 'Generalised Burgers equation for plane waves', J Acoust Soc Am 77, p2050 (1985)

[26] C W SMITH & R T BEYER, 'Ultrasonic radiation field of a focusing spherical source at finite amplitudes', J Acoust Soc Am 46, p806 (1969)

[27] E A ZABOLOTSKAYA & R V KHOKHLOV, 'Quasi-plane waves in the nonlinear acoustics of confined beams', Sov Phys Acoust 15, p35 (1969)

[28] V P KUZNETSOV, 'Equations of nonlinear acoustics', Sov Phys Acoust 16, p467 (1971)

[29] B G LUCAS & T G MUIR, 'Field of a finite amplitude focusing source', J Acoust Soc Am 74 p1522 (1983)

[30] S I AANONSEN, T BARKVE, J NAZE TJØTTA & S TJØTTA, 'Distortion and harmonic generation in the nearfield of a finite amplitude sound beam', J Acoust Soc Am 75, p749 (1984)

[31] A C BAKER, K ANASTASIADIS & V F HUMPHREY, 'The nonlinear pressure field of a plane circular piston: Theory and experiment', J Acoust Soc Am 84, p1483 (1988)

[32] A C BAKER, 'Nonlinear pressure fields due to focused circular apertures', J Acoust Soc Am 91 p713 (1992)

[33] A C BAKER & V F HUMPHREY, 'Distortion and high frequency generation due to nonlinear propagation of short ultrasonic pulses from a plane circular piston', to be published in J Acoust Soc Am (1992)

[34] P T CHRISTOPHER & K J PARKER, 'New approaches to nonlinear diffractive field propagation,' J Acoust Soc Am 90, p488 (1991)

[35] D DALECKI, E L CARSTENSEN, K J PARKER & D R BACON, 'Absorption of finite amplitude focused ultrasound', J Acoust Soc Am 89, p2435 (1991)

[36] M F HAMILTON, J NAZE TJØTTA & S TJØTTA, 'Nonlinear effects in the far-field of a directive sound source', J Acoust Soc Am 78, p202 (1985)

[37] S I AANONSEN 'Numerical computation of the nearfield of a finite amplitude sound beam', Rep. No. 73, Dept. of Mathematics, University of Bergen, Norway (1983)